Impulse Response Calibration of a Neutron Temporal Diagnostic

Using the Multi-Terawatt Laser

Matthew Wang

Pittsford Sutherland High School

Pittsford, NY

Advisor: Dr. Christian Stoeckl

Laboratory for Laser Energetics

University of Rochester

Rochester, New York

April 2016

Abstract

In inertial confinement fusion (ICF) experiments on OMEGA, the neutron production width is an important metric used to assess the quality of the implosions. In order to measure this width accurately, the impulse response of the neutron temporal diagnostic (NTD) system must be known precisely. The NTD uses a plastic scintillator that converts neutron energy into light, which is recorded by an optical streak camera capable of resolving temporal history. An NTD system was designed and built for the Multi-Terawatt (MTW) Laser, which uses x-ray pulses to simulate neutron production, in order to develop techniques to optimize its impulse response. The performance of this system was evaluated by varying the configuration of the laser, which included pulse duration, energy, focus condition, and target material, as well as by varying the NTD nose cone, which houses the scintillator. An important finding is that the measured impulse response using an aluminum nose cone was twice as fast as that using a tungsten nose cone. Techniques developed during this experiment will be used to optimize the impulse response of the NTD system on OMEGA.

I.   Introduction

Thermonuclear fusion, which does not generate nuclear waste, produces the most basic form of energy in the universe and has significant long-term application in the generation of electric power. One approach to controlled fusion, investigated at LLE, is ICF. In ICF experiments, shells are filled with either deuterium or deuterium-tritium mixtures and are compressed by direct laser illumination [1,2], soft x-ray radiation in a laser-heated hohlraum [3], or strong magnetic fields [4], resulting in thermonuclear fusion. As a measure of the quality of these experiments, the neutron production width must be known and recorded accurately [5]. However, the neutron temporal diagnostic (NTD) systems used to capture these events have a finite impulse response, which needs to be measured accurately. Impulse response, in this context, is defined as the width of the detected signal that results from an infinitesimally short pulse of neutrons. In this work, an NTD was designed and built for the MTW laser to develop techniques to optimize the impulse response of such systems. Although similar NTDs have been developed and implemented on larger lasers, including one on OMEGA, there are few shots readily available on the OMEGA laser system for experimentation. Thus, the brief cooldown time of the MTW laser, approximately half an hour, made it ideal for the experimentation conducted in this project.

II.   Experimental Setup

Figure 1 illustrates the experimental setup of the MTW-NTD system and the optical relay path from the target chamber to the streak camera. The optical relay path is composed of a scintillator, housed in the nose cone, a lens barrel, two mirrors, a filter, a focus lens, and an optical streak camera.
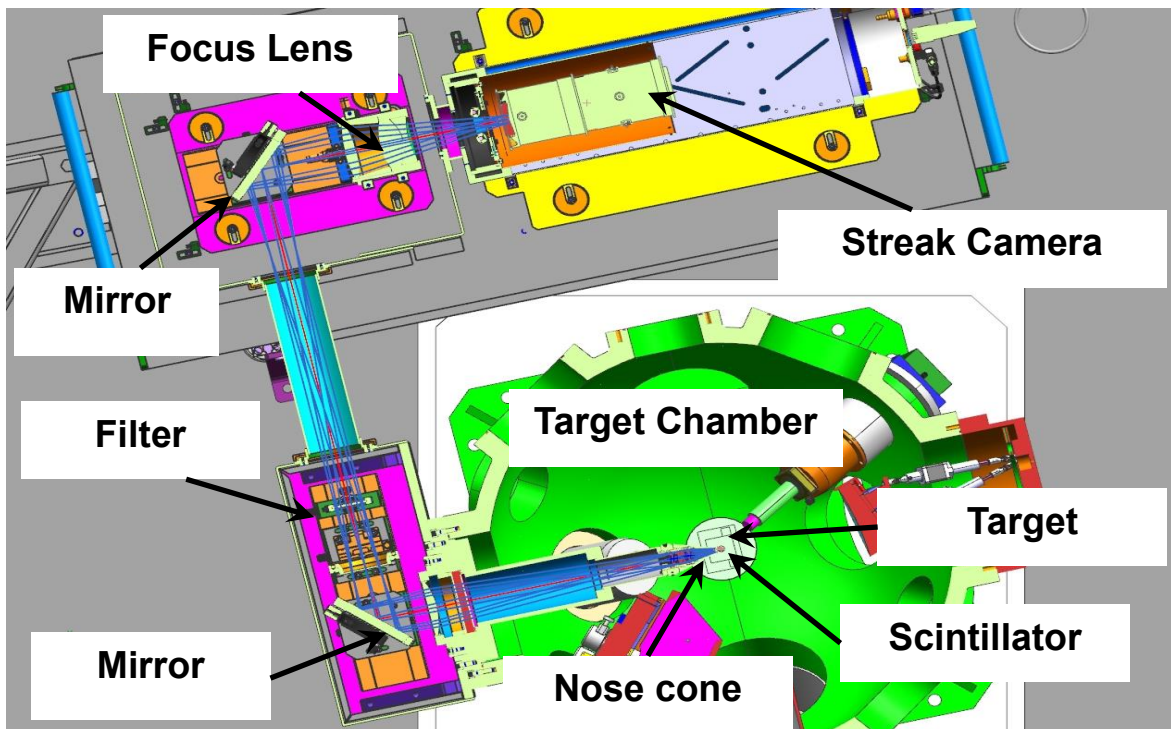

Fig. 1: *CAD drawing of the MTW-NTD experimental setup. X-ray energy produced from the interaction between the target material and the laser pulse is converted into light by the scintillator, housed in the nose cone.*

The targets used in this experiment included gold, copper, and aluminum targets, ranging from 500 by 500 by 3 microns to 500 by 500 by 20 microns. The x rays produced from the interaction of the MTW laser pulse with the target were converted into light by a BC-422 plastic scintillator, with a rise time determined to be less than 20

ps [6]. The light emitted by the scintillator traveled through the optical relay system, as illustrated in **Figure 1**, and ultimately was focused onto and recorded by an optical streak camera. **Figure 2**, from **Ref. 7**, describes the operation of a typical streak camera. The incident light on the photocathode is converted into electrons, the number of electrons being dependent on the intensity of the incident light for a given length of time. The electrons are accelerated by high voltage electrodes onto the phosphor screen, and are then converted back into light [7]. As the electrons pass through the streak tube, the voltage across the sweep electrodes is adjusted such that electrons that arrive at later times are deflected to a different spot on the phosphor screen, producing an image read by a CCD camera that is resolved in both the temporal and spatial directions.
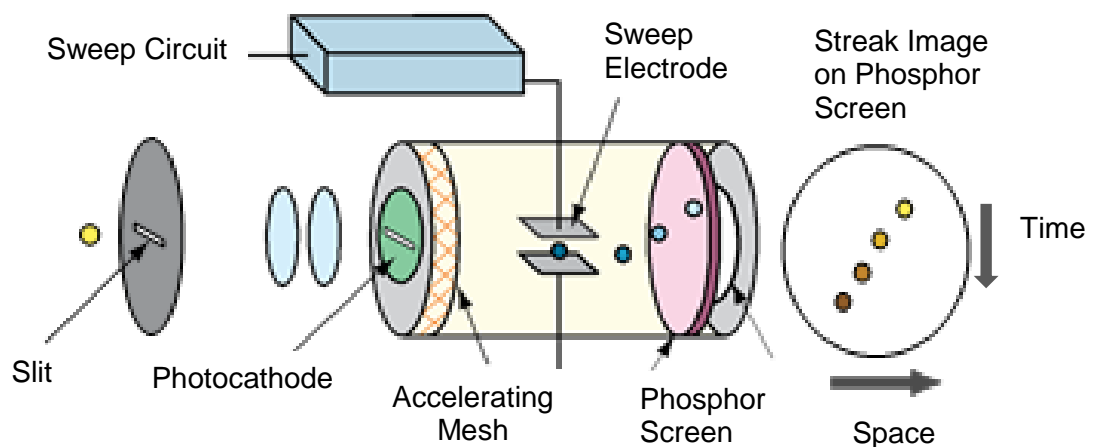

Fig. 2: Illustration of the components of an optical streak tube [7]. The optical streak camera is capable of converting incident light into electrons, which create an image on the phosphor screen after being deflected by the sweep electrodes.

LLE's ROSS P510 streak camera was used in this work. Extensive calibrations were performed for the streak camera, including correcting geometric distortions by

using a slow sweep, as well as calibration of the sweep speed and adjusting the initial biases of the electrodes to optimize focus [8].

III.   Data Collection

Over thirty shots of the MTW laser system were taken during a week of experimentation. **Figure 3** shows a CCD image produced from the first shot of the MTW-NTD laser and a corresponding lineout of intensity vs. space.
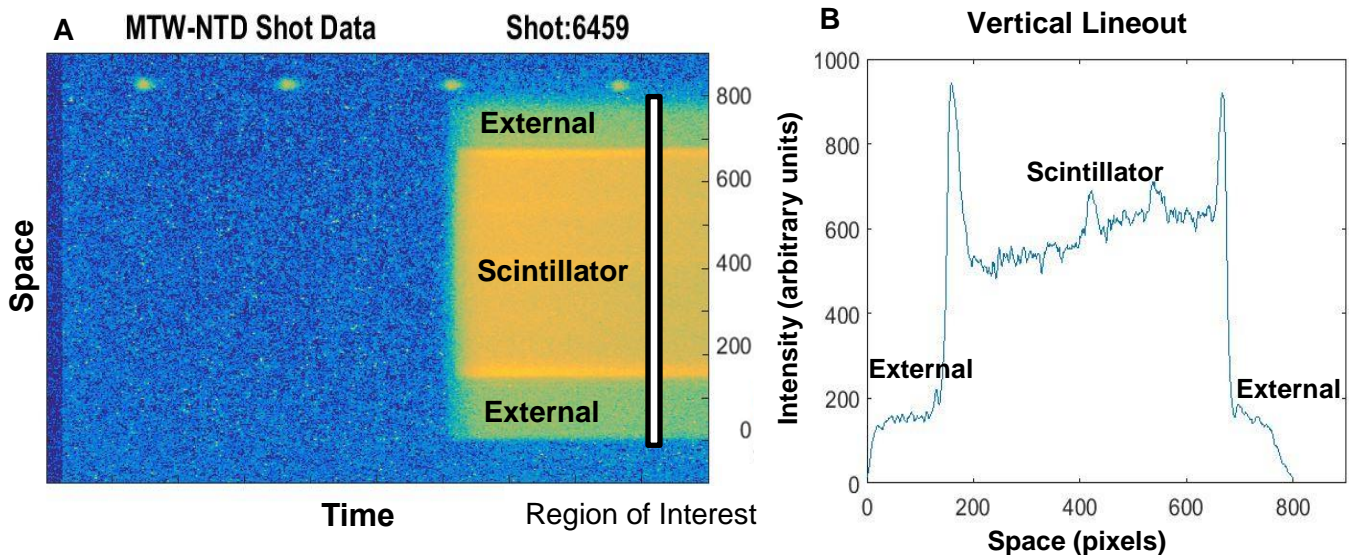

Fig. 3: (A) CCD image of the MTW laser shot. The x-axis indicates the temporal direction, while the y-axis represents the spatial direction. The brightness correlates to the intensity of the light produced. (B) Plot of the light intensity as a function of space. The external signal was associated with the presence of noise outside of the edges of the scintillator.

In **Figure 3A**, light produced from the scintillator is shown in the region from ~150 pixels to ~650 pixels on the y-axis. As shown in the image, around 850 pixels on the y-axis, a fiducial pulse of 506 ps was used to calibrate the time elapsed per pixel. The data reveals an unexpected signal produced from the region outside the scintillator, shown in the picture to be from 0 to ~150 pixels and from ~700 to ~800 pixels.

Furthermore, from **Figure 3B**, the plot indicated that the external signal was about 1/4 the intensity of the main signal. Another finding that was made from the first shot was regarding the leading edge of the scintillator signal. From the image a green-blue stripe could be seen before the characteristic orange-yellow scintillator signal.

As a result of these initial findings, subsequent changes in the experimental configuration were made to further investigate the sources of the external signal and the leading edge of the signal, ultimately to see if they would have an effect on the impulse response of the MTW-NTD system.

A. Cherenkov Radiation

Three shots were taken with an alignment nose cone. Since this nose cone did not contain a scintillator at the bottom, the resulting image should have revealed no signal. **Figure 4** shows the image produced from one of the alignment nose cone shots.
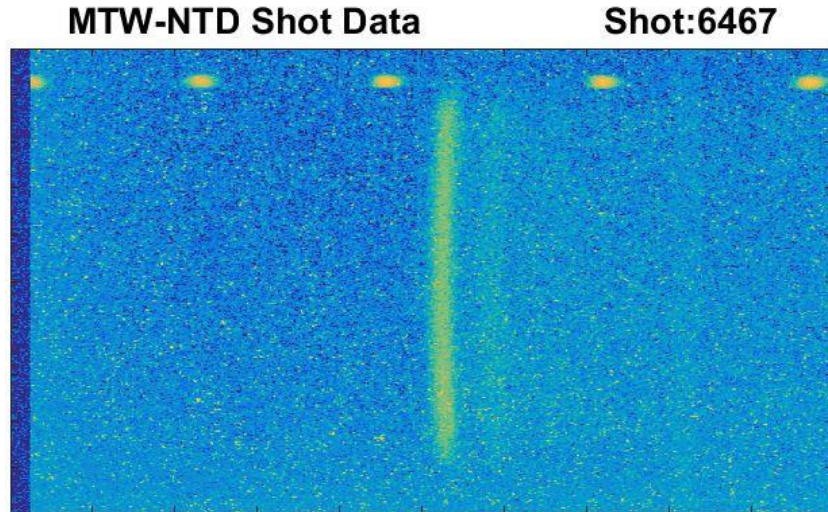
Fig. 4: *CCD image of an MTW laser shot with the alignment nose cone (no scintillator).*

The image indicated that a signal was still present even though there was no scintillator in the alignment nose cone. It was determined that this signal was produced from Cherenkov radiation in the nose cone lenses. Cherenkov radiation is light emitted from an electron when the electron travels through a medium faster than the phase velocity of light in that medium. As the production of energetic elections is highly dependent on the laser intensity, other shots were taken with the alignment nose cone but with the laser defocused, to see if the intensity of the Cherenkov radiation would be affected. The laser was defocused by 50 μm and by 100 μm, and the corresponding intensity of the Cherenkov radiation is shown in **Figure 5**.
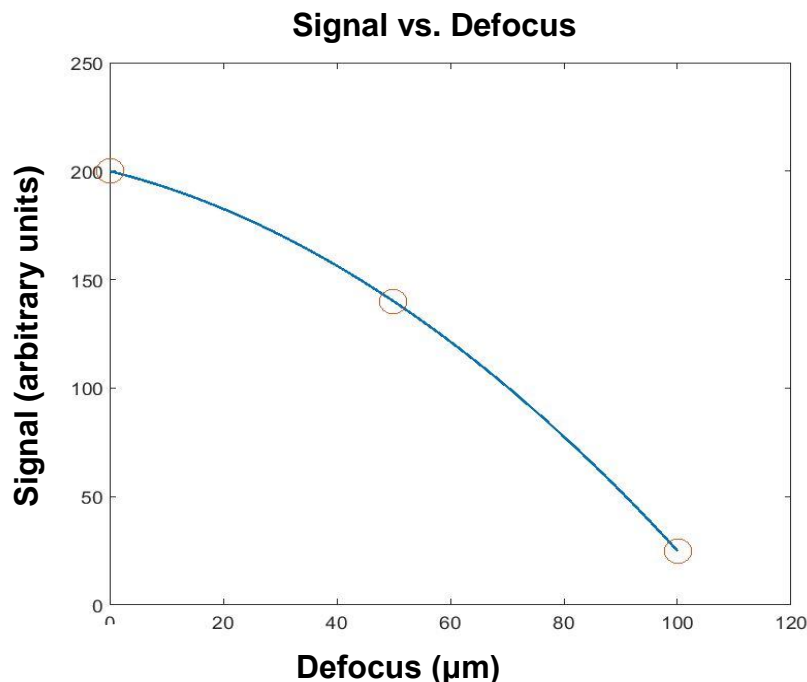
Signal vs. Defocus

Fig. 5: *Plot of the signal intensity vs. defocus. These shots confirmed the presence of Cherenkov radiation.*

From these shots it was found that the intensity of the Cherenkov radiation could be significantly reduced by defocusing the laser by 100 μm. As a result, subsequent shots were taken with the laser defocused by 100 μm.

B. External Signal

The external signal shown in **Figure 3A** was found to have been the result of scintillator light reflecting off the surface of the nose cone, as illustrated in **Figure 6**. The nose cones were then coated with a less reflective material, black plastic foil, which was shown to reduce the intensity of the external signal, as shown in **Figure 7**.

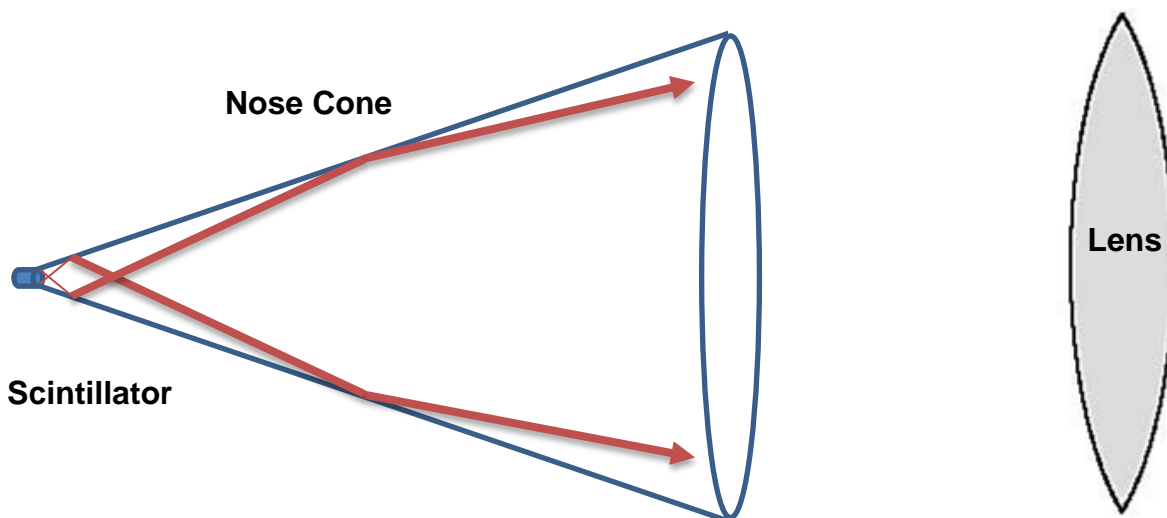**Nose Cone**

Lens

Scintillator

*Fig 6: Schematic of the origin of the external signal produced by the scintillator and nose cone (enlarged). Light rays that reflected off the nose cone were not focused correctly and produced an external signal, shown in **Figure 3b**.*
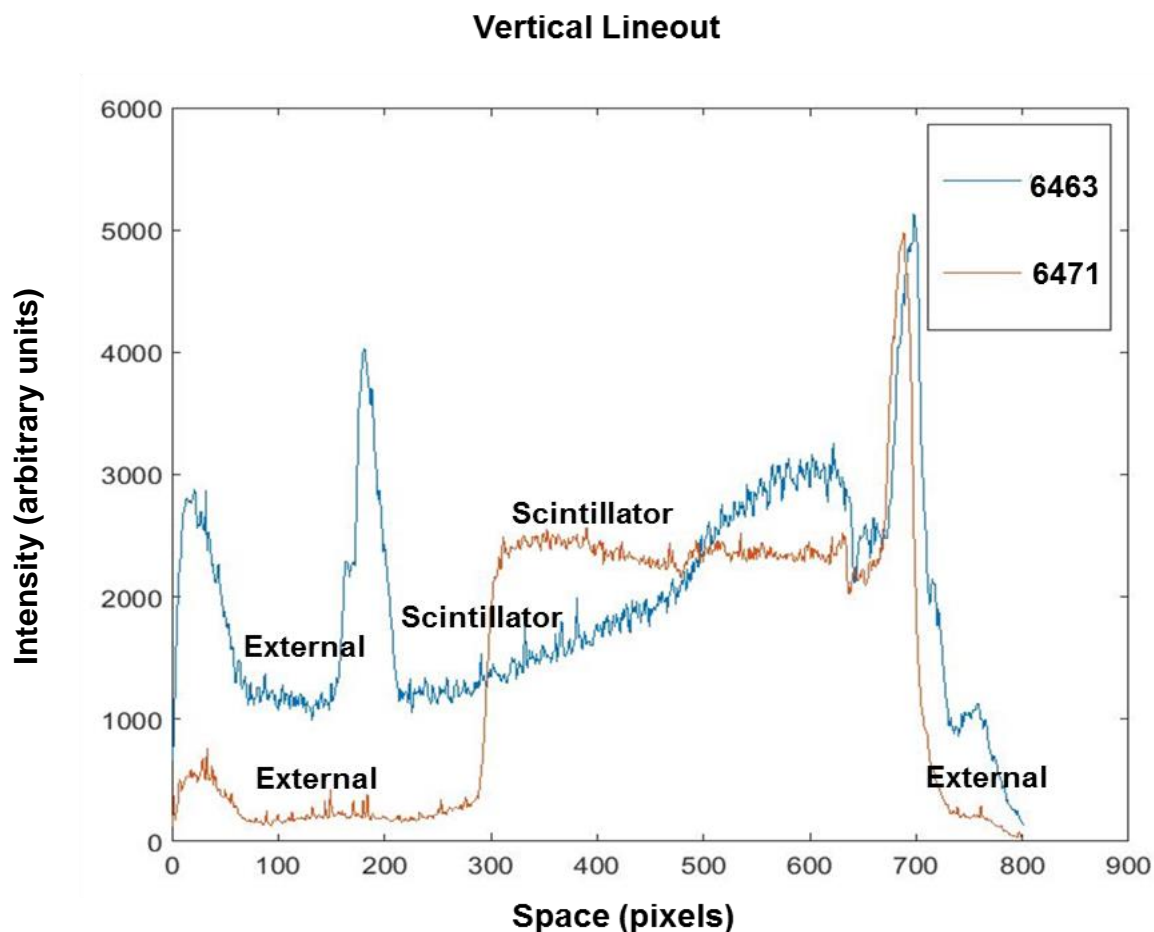
Fig. 7: *Plot of the intensity vs. space for shots 6463 and 6471, one of which (Shot 6471) was taken with the nose cone coated with a less reflective surface. The external signal was significantly reduced in Shot 6471.*

The ratio of the external signal from shot 6463, in the region ~75-150 pixels, to the scintillator signal, in the region ~200-675 pixels, is ~1:1.5. Compared to that for shot 6471, which indicated a ratio of the external to scintillator signal of ~1:8, the less reflective coating significantly reduced the amount of reflected scintillator light. After this finding all subsequent shots were taken with the nose cone coated with the black plastic foil.

IV.   Data Analysis

A. Physical Modeling Equation

A physical modeling approach was used to remove the effect of the long scintillator decay. The equation is given by

$$N_i = S_i - \sum_{j=0}^{i-1} N_j \exp\left[\frac{-(i-j) \times \Delta t_p}{d}\right] \tag{1}$$

where the signal at pixel location i, N_i, is given as the recorded signal S_i minus the sum of all earlier neutron signals, which decay exponentially at the scintillator fall time d, with Δt_p as the time separation of the two pixels [5]. In this work 1.4 ns was used as the scintillator fall time. The deconvolution of the signal can be seen in **Figure 8**.
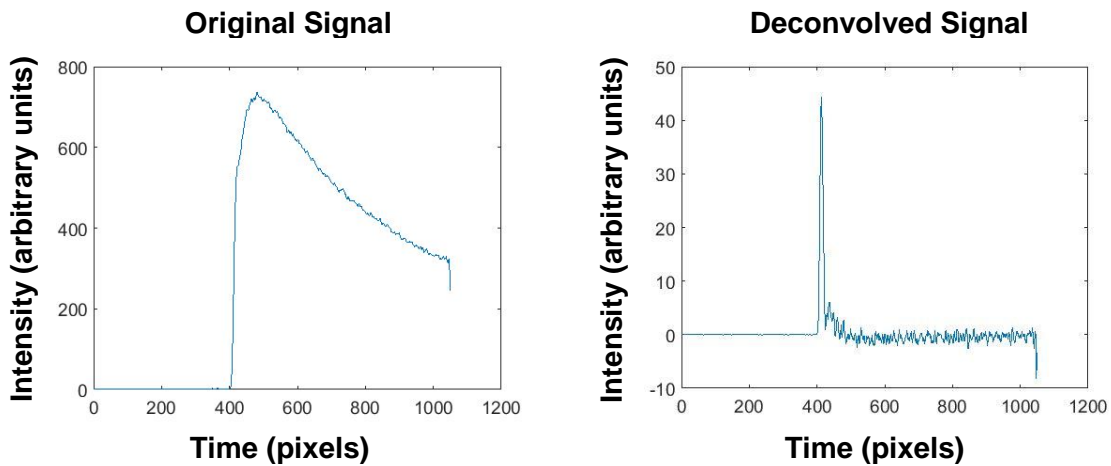

Fig. 8: Horizontal plots of the signal intensity vs. time. The deconvolution of the original signal produces an unfolded signal whose full width half maximum (~22 ps) could be determined.

A Gaussian fit was used to measure the full width half maximum (FWHM) of the unfolded signal in order to determine the impulse response of the MTW-NTD system.

B. Experimental Findings

The most significant finding from this experiment was that an aluminum nose cone produced a shorter impulse response compared to that for a tungsten nose cone. **Figure 9** shows the comparison of the tungsten and aluminum nose cones used in this work.
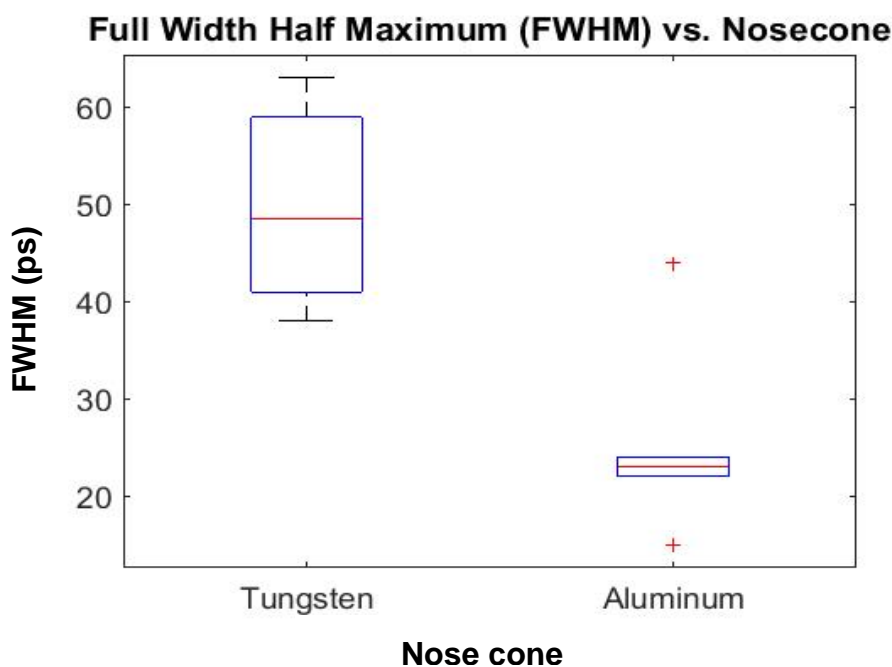

Fig. 9: *Box plot comparing the impulse response for the aluminum and tungsten nose cones. The aluminum nose cone impulse response was measured to be twice as fast as the tungsten nose cone. (The "+" signs in the data for the aluminum nose cone represent experimental outliers)*

The aluminum nose cone was measured to produce an impulse response of ~25 ± 2 ps, and the tungsten nose cone an impulse response of ~50 ± 10 ps. Besides nose

cone material, several parameters of the MTW-NTD setup were adjusted, including target material, pulse duration, defocus, and energy. As there were several parameters that differed between shots and since only thirty shots were taken, it was difficult to compare a significant number of shots that differed in only a single parameter.

Another finding that was made in this experiment was that the impulse response of the system using the aluminum nose cone was more consistent with a short pulse duration, shown in **Figure 10**. Although the average measured impulse response was ~23-25 ps for the two laser pulse durations, with a laser pulse ~1 ps, the range was measured to be ~4 ps, whereas with a laser pulse ~10 ps, the range was measured to be ~30 ps.
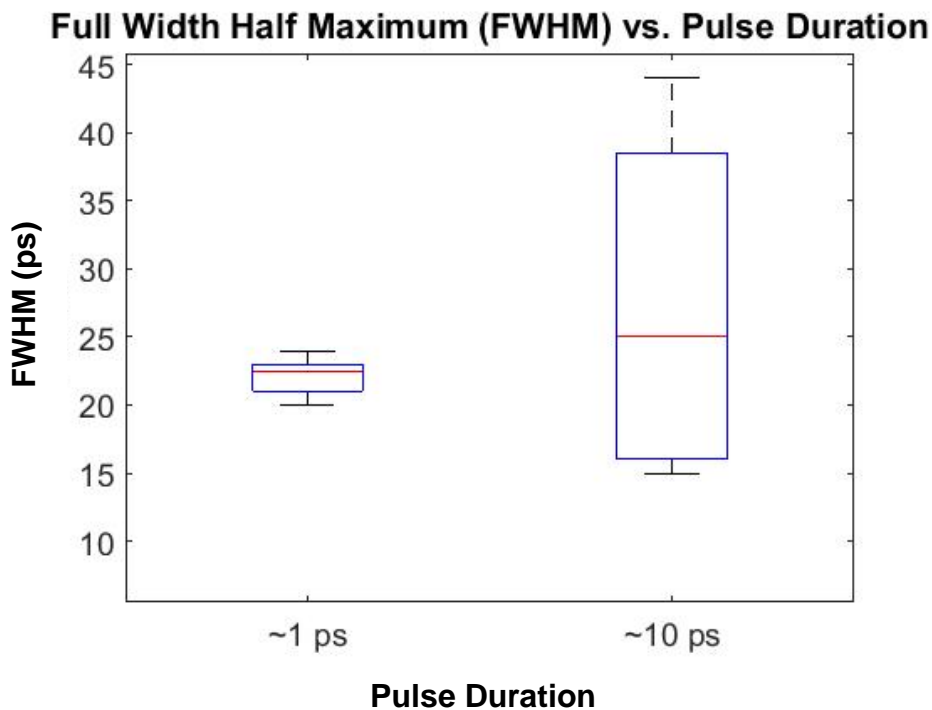
Full Width Half Maximum (FWHM) vs. Pulse Duration

***Fig. 10:** Box plot of FWHM vs. Pulse Duration for the aluminum nose cone. The shorter pulse duration of the MTW laser system produced a more consistent impulse response.*

Another notable finding of this experiment was the effect of defocusing the laser on the system performance, as shown in **Figure 11**. Although there were few shots with which to directly compare the effects of defocus on the measured impulse response, the defocused laser did produce a faster average impulse response, ~37 ± 2 ps compared to ~55 ± 1 ps. This suggests that the Cherenkov radiation had a negative impact on the MTW-NTD system performance, as its intensity without any defocus was ~200 units, and with 100 µm defocus it was ~20 units (see **Figure 5**).

Full Width Half Maximum (FWHM) vs. Defocus

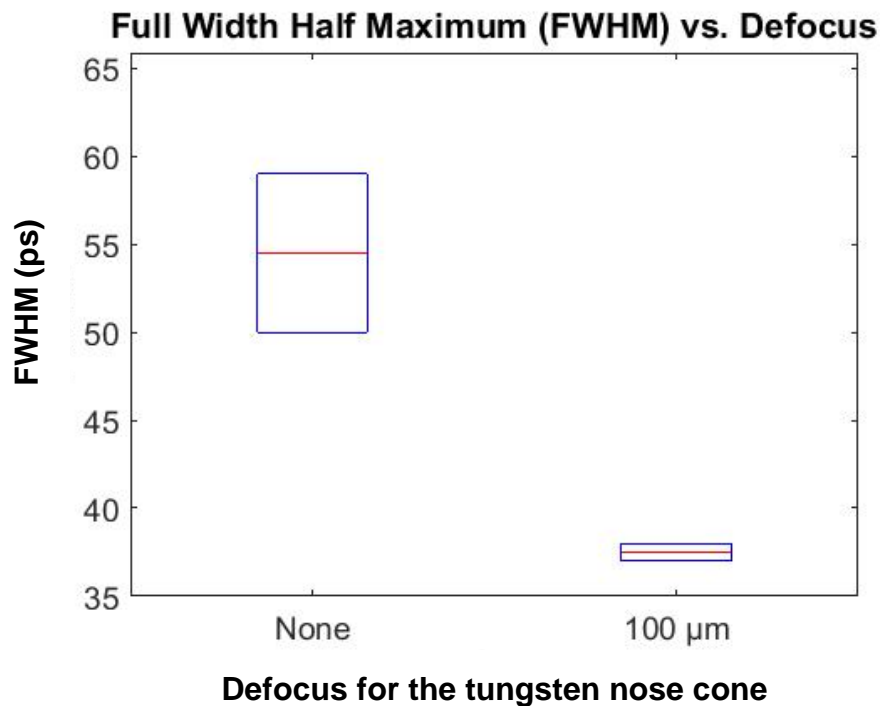**Defocus for the tungsten nose cone**

*Fig. 11: Box plot of the FWHM vs. Defocus for the tungsten
nose cone. Defocusing the laser by 100 μm produced a faster
and more consistent MTW-NTD impulse response.*

Several adjustments made to the MTW setup yielded insignificant changes to the

NTD performance. Some of these included the energy of the MTW laser shot, the target

material, and the plastic nose cone coating. The lack of dependence on the coating

indicated that the reflected light had very little effect on the measured impulse response

of the system.

V.   Conclusions

A NTD system was designed and built for experimentation on the MTW laser system to develop techniques for optimizing the impulse response. During the data collection, Cherenkov radiation and an external signal were discovered in the CCD images. The intensity of both were reduced by defocusing the laser and by coating the nose cone with a less reflective surface. Cherenkov radiation was found to increase the measured system impulse response time, while the external signal had little effect on the response time. The most notable finding of this work is that the aluminum nose cone produced an impulse response of ~25 ps, whereas the tungsten nose cone produced an impulse response of ~50 ps. Many alterations in parameters, including laser energy and target material, yielded little improvement in system performance. Further investigations will be conducted to confirm and expand upon these findings, and ultimately such techniques will be implemented for use on OMEGA.

VI.   Acknowledgements

I would like to thank my advisor, Dr. Stoeckl, for encouraging me to ask questions about the theory underlying the research as well as for his support and guidance in each phase of the project. Dr. Stoeckl's unwavering enthusiasm helped me gain a considerably better understanding of the physics and theoretical background regarding the experiment. Also, many thanks to Joe Katz, whose help with hardware and the MTW-NTD assembly was instrumental to the project's success. Also, Joe's involvement with the project was extremely helpful, especially during the first week of the research when Dr. Stoeckl was unavailable.

I would like to thank Dr. Craxton for his work in providing us the resources and for helping guide us through the brief eight weeks of research. It is a testament to Dr. Craxton's tremendous efforts that this high school program has been so successful in educating high school students for so many years.

Finally, I would like to thank my fellow interns for their help and for creating a relaxed work environment. I especially wish to thank Jonah Simpson, whose assistance with writing the Matlab code was extremely helpful in compiling and analyzing the data.

VII. References

1. J. Nuckolls, L. Wood, A. Thiessen, and G. Zimmerman, " Laser compression of matter to super-high densities: Thermonuclear (CTR) applications," Nature 239, 139 (1972).

2. R. S. Craxton, K. S. Anderson, T. R. Boehly, V. N. Goncharov, D. R. Harding, J. P. Knauer, R. L. McCrory, P. W. McKenty, D. D. Meyerhofer, J. F. Myatt, A. J. Schmitt, J. D. Sethian, R. W. Short, S. Skupsky, W. Theobald, W. L. Kruer, K. Tanaka, R. Betti, T. J. B. Collins, J. A. Delettrez, S. X. Hu, J. A. Marozas, A. V. Maximov, D. T. Michel, P. B. Radha, S. P. Regan, T. C. Sangster, W. Seka, A. A. Solodov, J. M. Soures, C. Stoeckl, and J. D. Zuegel, "Direct-Drive Inertial Confinement Fusion: A Review," Phys. Plasmas 22 (11), 110501 (2015).

3. J. D. Lindl, " Development of the indirect-drive approach to inertial confinement fusion and the target physics basis for ignition and gain," Phys. Plasmas 2, 3933 (1995).

4. S. A. Slutz, M. C. Herrmann, R. A. Vesey, A. B. Sefkow, D. B. Sinars, D. C. Rovang, K. J. Peterson, and M. E. Cuneo, "Pulsed-Power-Driven Cylindrical Liner Implosions of Laser Preheated Fuel Magnetized with an Axial Field," Phys. Plasmas **17** (5), 056303 (2010).

5. Stoeckl, C., et al. "Neutron temporal diagnostic for high-yield deuterium–tritium cryogenic implosions on OMEGA." *Review of Scientific Instruments* 87 (2016): 053501.

6. Lerche, R. A., and D. W. Phillon. "Rise time of BC-422 plastic scintillator< 20 ps." Nuclear Science Symposium and Medical Imaging Conference, 1991., Conference Record of the 1991 IEEE. IEEE, 1991.

7. *Guide to Streak Cameras*. Hamamatsu Photonics K.K., 2008. https://www.hamamatsu.com/resources/pdf/sys/SHSS0006E_STREAK.pdf

8. Donaldson, W. R., et al. "A self-calibrating, multichannel streak camera for inertial confinement fusion applications." Review of Scientific Instruments 73 (2002): 2606-2615.